ELSEVIER

Biochimica et Biophysica Acta 1228 (1995) 189–200

BBA Biochimica et Biophysica Acta

Direct detection of a carboxylate bridge between Mn and Ca^{2+} in the photosynthetic oxygen-evolving center by means of Fourier transform infrared spectroscopy

Takumi Noguchi *, Taka-aki Ono, Yorinao Inoue

Solar Energy Research Group, The Institute of Physical and Chemical Research (RIKEN), Wako, Saitama 351-01, Japan

Received 8 September 1994; accepted 4 November 1994

Abstract

Calcium is an indispensable cofactor for photosynthetic oxygen evolution. We have studied structural relevance of Ca^{2+} to the oxygen-evolving center (OEC) of Photosystem II (PS II) by means of Fourier transform infrared (FTIR) spectroscopy. The single-pulse induced FTIR difference spectra of PS II membranes reflecting solely the structural changes of OEC between in the S_1 and S_2 states were measured by controlling the redox potential and pH of the buffer. Comparison between the two S_2/S_1 difference spectra using untreated and Ca^{2+}-depleted PS II membranes showed that the negative bands at 1560 and 1403 cm^{-1} (belonging to S_1) and the positive bands at 1587 and 1364 cm^{-1} (belonging to S_2) were lost upon Ca^{2+} depletion. These bands were assigned to the asymmetric (higher frequency bands) and symmetric (lower frequency bands) COO^- stretching modes of a certain carboxylate group in Asp, Glu or the C-termini, based on the infrared data of 20 amino acids and the S_2/S_1 spectra of ^{15}N-labeled PS II membranes. The frequency differences of the asymmetric and symmetric COO^- bands, i.e., 157 cm^{-1} for S_1 and 223 cm^{-1} for S_2, indicated that this carboxylate group possesses the structure of bridging bidentate coordination in the S_1 state and that of unidentate coordination in the S_2 state. Taking together the observation of disappearance of these bands upon Ca^{2+} depletion, it was concluded that (i) this carboxylate serves as a bridging ligand between the redox-active Mn and the Ca^{2+} ions, (ii) upon S_2 formation, the coordination bond of this carboxylate to Ca^{2+} is selectively broken, and (iii) upon depletion of Ca^{2+}, this carboxylate ligand is liberated even from the Mn ion. Along with the changes of COO^- bands, several intense bands in 1680–1630 cm^{-1}, which were assigned to the amide I modes of backbone amide groups, were lost upon Ca^{2+} depletion. This indicates that some perturbations on the protein conformations around the Mn-cluster induced by the S_2 formation require the presence of Ca^{2+} in OEC. Possible roles of Ca^{2+} in the oxygen-evolving reactions are discussed based on these findings.

Keywords: Photosystem II; Oxygen evolution; FTIR; Carboxylate ligand; Manganese cluster

1. Introduction

Oxygen, indispensable for almost all life on the earth, is produced by plants as a product of water oxidation in photosynthetic processes. The active site of the reaction, the oxygen-evolving center (OEC), is thought to consist of four Mn ions, the so-called Mn-cluster, residing on the lumenal side of Photosystem II (PS II). The reaction proceeds through the S-state cycle [1,2]: single-electron oxidation of OEC advances the S_i ($i = 0$–3) state to the next S-state. The S_1 state is a thermally stable state, and oxygen release occurs upon S_3-to-S_0 transition (for a recent review, see [3]).

Extensive studies by means of X-ray absorption spectroscopy and electron paramagnetic resonance (EPR), both of which can detect direct signals from the Mn ions, have provided some structural images of the Mn-cluster, i.e., a multinuclear cluster in which the Mn ions are coupled through μ_2-oxo-bridges (reviewed in [3,4]). As for the protein structure in OEC including amino-acid ligands, however, these spectroscopies provided only limited infor-

Abbreviations: DCMU, 3-(3,4-dichlorophenyl)-1,1-dimethylurea; ENDOR, electron nuclear double resonance; EPR, electron paramagnetic resonance; ESEEM, electron spin echo envelope modulation; EXAFS, extended X-ray absorption fine structure; FTIR, Fourier transform infrared; IR, Infrared; Mes, 2-(N-morpholino)ethanesulfonic acid; Mops, 3-(*N*-morpholino)propanesulfonic acid; OEC, oxygen-evolving center; PS II, Photosystem II; Q_A, primary quinone acceptor in Photosystem II; Q_B, secondary quinone acceptor in Photosystem II, XANES, X-ray absorption near-edge structure

* Corresponding author. Fax: +81 48 4624685.

SSDI 0005-2728(94)00171-5

mation; a few nitrogen atoms coordinated to Mn were revealed by electron spin echo envelope modulation (ESEEM) [5,6] and electron nuclear double resonance (ENDOR) [7] studies.

Calcium is known as an essential cofactor for oxygen evolution (reviewed in [3,8]). Depletion of Ca^{2+} inactivates oxygen evolution and readdition of Ca^{2+} restores the activity. It is thought that in Ca^{2+}-depleted PS II, the transition from S_2 to S_3 [9,10] or that from S_3 to S_0 [11,12] is blocked. The binding site of Ca^{2+} in PS II has not been identified yet [8], although Ca^{2+} is thought to be located in the close vicinity of the Mn-cluster [10,11,13,14]. The specific role of Ca^{2+} in the oxygen-evolving reaction is still an open question.

Recently, we have studied the structure of OEC by means of light-induced FTIR difference spectroscopy, which provides direct signals from the protein moieties around the Mn-cluster [15–17]. The FTIR difference spectra specific to OEC between its S_1 and S_2 states were successfully obtained by using trypsinized PS II membranes in the presence of an exogenous electron acceptor to eliminate the acceptor-side signals [15,16]. The temperature dependence of the band appearance, which was identical with that of the S_2 formation, further confirmed that the obtained FTIR signals were due to the changes upon S_1-to-S_2 transition [17]. The prominent bands in the spectra have been tentatively assigned to the COO^- stretching modes arising from the carboxylate ligands of the redox-active Mn ions and to the amide I modes reflecting conformational changes in the protein around the Mn-cluster [15–17].

In this paper, we report the structural relevance of Ca^{2+} to OEC as studied by FTIR spectroscopy. The S_2/S_1 difference spectra of OEC measured with untreated and Ca^{2+}-depleted PS II membranes have provided the first evidence for the presence of a carboxylate bridge between Mn and Ca^{2+}. The results have also shown that upon S_2 formation, this bridging carboxylate undergoes breakage of the coordination bond to Ca^{2+} accompanied by protein conformational changes. Implication of these structural changes relevant to Ca^{2+} is discussed in regard with the oxygen-evolving reactions.

2. Materials and methods

BBY-type PS II membranes [18] capable of O_2 evolution were prepared from spinach according to Ono and Inoue [19]. Spinach whose nitrogen atoms were replaced by ^{15}N was cultured by hydroponics with a medium containing $K^{15}NO_3$ (99.8%, Shoko Co.) and $Ca(^{15}NO_3)_2$ (99.5%, Shoko Co.) as nitrogen sources. The PS II membranes were suspended in Mes-NaOH buffer (400 mM sucrose, 20 mM NaCl, 20 mM $CaCl_2$, 40 mM Mes (pH 6.5)), and incubated on ice in darkness overnight to make every OEC relax to the thermally stable S_1 state.

Depletion of Ca^{2+} was preformed by low-pH treatment as described by Ono et al. [20]. The membranes were suspended with 400 mM sucrose, 20 mM NaCl and 10 mM citrate-NaOH (pH 3.0) and incubated on ice for 5 min, followed by addition of 0.1 volume of 400 mM sucrose, 20 mM NaCl and 500 mM Mops-NaOH (pH 7.5). The sample suspension was further incubated on ice for 20 min to facilitate the rebinding of the extrinsic 24 and 16 kDa proteins. All the procedures for Ca^{2+} depletion were performed in darkness so that the relatively stable Ca^{2+}-depleted S_2 state was not accumulated. Restoration of Ca^{2+} was done by resuspending the Ca^{2+}-depleted PS II membranes in the Mes-NaOH buffer that contained 20 mM $CaCl_2$, and by subsequent dark incubation for 30 min on ice. Mn-depleted PS II membranes were prepared by NH_2OH treatment as reported previously [15].

For FTIR measurements, the PS II sample was resuspended with the buffer specified for each measurement with the concentration of 0.5 mg chlorophyll/ml. For an S_2/S_1 difference spectrum of untreated PS II membranes, the used buffer was 40 mM Mes-NaOH (pH 5.5), 400 mM sucrose, 20 mM NaCl, 20 mM $CaCl_2$, 18 mM potassium ferrocyanide, and 2 mM potassium ferricyanide. For an S_2/S_1 spectrum of Ca^{2+}-depleted PS II membranes, the buffer was the same as the above one except for including 0.5 mM EDTA instead of 20 mM $CaCl_2$. For $S_2Q_A^-/S_1Q_A$ and Q_A^-/Q_A difference spectra, untreated PS II membranes and Mn-depleted PS II membranes, respectively, were suspended in 40 mM Mes-NaOH (pH 6.5), 400 mM sucrose, 20 mM NaCl, and 0.1 mM DCMU. For a Q_A^-/Q_A spectrum, 10 mM NH_2OH as an exogenous electron acceptor was further added in the above buffer. The sample suspension was centrifuged (150000g for 30 min), and the resultant membrane pellet was pressed between a pair of BaF_2 plates (13 mm ϕ). The sample temperature was controlled at 250 K in a cryostat (Oxford DN1704) with a temperature controller (Oxford ITC-4).

FTIR spectra of PS II samples were measured on a JEOL JIR-6500 spectrophotometer equipped with an MCT detector (EG & G JUDSON IR-DET101). A Ge filter (OCLI LO2584-9) was placed in front of the sample to block the He-Ne laser beam partially leaking into the sample room. Light-induced difference spectra were obtained by subtraction between the two single-beam spectra measured before and after illumination. Each single-beam spectrum was an average of 300 scans (150 s accumulation). For final data, several difference spectra were measured using different samples (each sample was illuminated only once) and were averaged. The S_2/S_1 spectra were smoothed by the Savitzky-Golay method in the JEOL software over five data points. The spectral resolution was 4 cm^{-1}. Light illumination was performed with a single pulse from a frequency-doubled (532 nm) Nd:YAG laser (Quanta-Ray DCR-1) having a pulse width of about 7 ns and an energy of about 10 mJ/pulse cm^2 on the sample surface (for S_2/S_1 spectra), or with continuous light from a tungsten lamp through

a red glass filter (> 620 nm) and heat-cut filters with an intensity of about 20 mW/cm^2 (for $S_2Q_A^-/S_1Q_A$ and Q_A^-/Q_A spectra).

FTIR spectra of all 20 L-amino acids were measured at room temperature with a TGS detector. Each amino acid was dissolved both in H_2O and in 1 M HCl solution (1–3%). Tyr was dissolved only in HCl solution, because this is almost insoluble in water. For Asp and Glu, their monosodium salts were used, and for Lys and Arg, their monohydrochloride salts were used. Spectra of thus prepared amino-acid solutions were measured between a pair of ZnSe plates with an about 6 μm spacer. A large water band around 1643 cm^{-1} was subtracted using the spectra of only water and 1 M HCl solution so that a natural baseline was obtained. It is noted that, although selection of a subtraction factor may be critical for the precise analysis of the bands in 1700–1600 cm^{-1}, it little affects the analysis of the bands lower than 1500 cm^{-1} which is our purpose in this study.

Redox potential (E_h) of the buffer was measured using a combined electrode (Horiba 6810-06T) connected to a pH meter (Horiba M-7 II).

3. Results

3.1. S_2/S_1 difference spectrum of untreated PS II membranes

Fig. 1A shows a single-pulse induced FTIR difference spectrum of untreated PS II membranes in a buffer at pH 5.5 containing a mixture of ferricyanide and ferrocyanide (1:9) measured at 250 K. In order to obtain an FTIR difference spectrum that is exclusively due to the S_2/S_1 changes in OEC, signals from the acceptor side of PS II must be eliminated. Although ferricyanide works as an exogenous electron acceptor, it also oxidizes the non-heme iron and generates an additional endogenous electron acceptor [21]. In fact, a single-pulse induced FTIR spectrum of untreated PS II membranes in the buffer (pH 6.5) with only ferricyanide (spectrum not shown) showed strong bands at 1659, 1338, 1259, 1227 and 1103 cm^{-1}, which can be ascribed to the non-heme iron signals (Fe(II)/Fe(III)) [22], along with the S_2/S_1 signals of OEC. To avoid the preoxidation of the non − heme iron, the redox potential (E_h) and pH (lower pH increases the midpoint potential of the non-heme iron) of the buffer medium should be controlled [21]. The E_h value of the Mes buffer (pH 5.5) including 18 mM potassium ferrocyanide and 2 mM potassium ferricyanide was 364 mV, at which the non-heme iron should stay reduced at pH 5.5 [21]. We note here that OEC is fully active at this pH value [23].

The S_2/S_1 FTIR spectrum obtained under these conditions (Fig. 1A) was almost completely free from the non-heme iron signals, as judged by the Fe(II)/Fe(III)

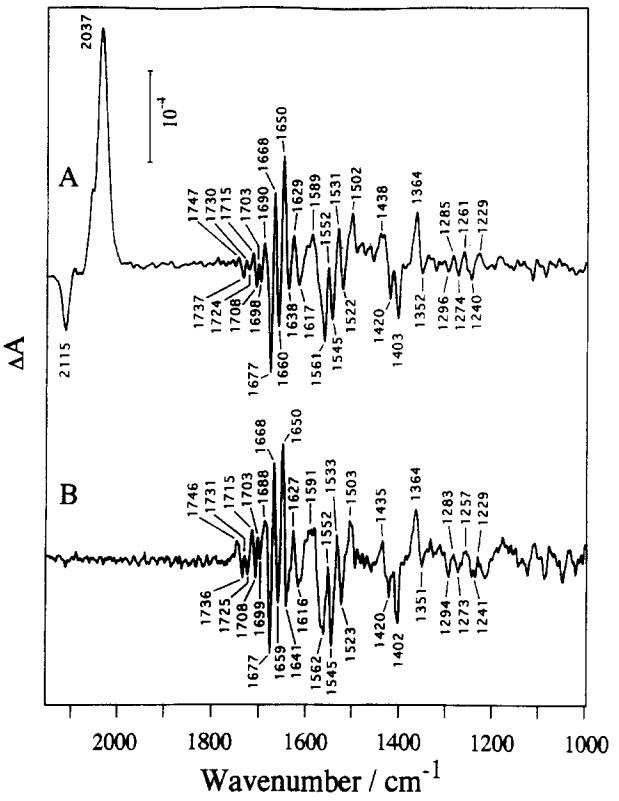

Fig. 1. (A) Single-pulse induced S_2/S_1 FTIR difference spectrum measured at 250 K with untreated PS II membranes in the Mes buffer (pH 5.5) in the presence of 2 mM potassium ferricyanide and 18 mM potassium ferrocyanide. A single pulse from a frequency-doubled (532 nm) Nd:YAG laser ($\approx$ 7 ns, 10 mJ) was used for illumination. Five spectra with different samples were averaged. (B) Double difference spectrum calculated by subtracting the Q_A^-/Q_A difference spectrum from the $S_2Q_A^-/S_1Q_A$ spectrum. The $S_2Q_A^-/S_1Q_A$ and Q_A^-/Q_A spectra were measured at 250 K with untreated and Mn-depleted PS II membranes, respectively, in the Mes buffer (pH 6.5) including 0.1 mM DCMU. For the Q_A^-/Q_A spectrum, 10 mM NH_2OH was further added as an exogenous electron donor. Continuous light from a tungsten lamp was used for illumination. Two spectra were averaged.

only spectrum reported by Hienerwadel et al. [22] and our S_2Fe(II)/S_1Fe(III) spectrum (not shown). Also, absence of the Q_A^-/Q_A signals represented by a strong positive band at 1478 cm^{-1} [15,17,24] means no contribution of the Q_A change to the spectrum. The strong positive ferrocyanide band at 2037 cm^{-1} (Fig. 1A) indicates that an electron is in fact abstracted from PS II by ferricyanide. It should be noted that our previous S_2/S_1 spectra [15,16] measured with trypsinized PS II membranes in the buffer (pH 6.5) containing only ferricyanide exhibited partial contribution of the non-heme iron signals. This means that trypsinization, which breaks the protein moiety around the Q_B binding site and enables direct abstraction of an electron from Q_A^- by exogenous electron acceptor [25], was not enough for complete elimination of the acceptor-side signals. However, the present study showed that an S_2/S_1 spectrum without any contribution of acceptor-side signals

can be obtained by controlling the redox potential and pH of the buffer using untreated PS II membranes.

The assignment of the spectrum of Fig. 1A as exclusively due to the S_2/S_1 changes was further confirmed by Fig. 1B, a double difference spectrum between the $S_2Q_A^-/S_1Q_A$ and Q_A^-/Q_A spectra. The former and the latter spectra were obtained as the difference between before and after continuous-light illumination of untreated PS II membranes and Mn-depleted PS II membranes, respectively, in a pH 6.5 buffer including DCMU [15]. Subtraction of the latter from the former would eliminate the Q_A^-/Q_A signals, and give the difference signals only due to S_2/S_1 changes. Notably, the two spectra (Figs. 1A and 1B) almost completely agree with each other in the 1800–1000 cm^{-1} region, supporting our idea that the spectrum in Fig. 1A is exclusively derived from the changes in OEC with no contamination of acceptor-side signals. The agreement of the two spectra also indicates that the OEC does not change its structure between pH 5.5 and pH 6.5, consistent with the full activity of oxygen evolution at pH 5.5 [23].

3.2. S_2/S_1 difference spectrum of Ca^{2+}-depleted PS II membranes

Fig. 2 compares the single-pulse induced FTIR difference spectrum of Ca^{2+}-depleted PS II membranes (Fig. 2B) to that of untreated PS II membranes (Fig. 2A). Since Ca^{2+} depletion was performed by low-pH treatment in the dark [20], the Ca^{2+}-depleted OEC thus prepared is in its S_1 state. In fact, Ca^{2+}-depleted PS II membranes prepared with the same procedures did not show any multiline EPR signal in the dark, whereas illumination of this sample generated the multiline signal indicative of the formation of the Ca^{2+}-depleted S_2 state [26]. Also, in our X-ray absorption near edge structure (XANES) study [27] using the same Ca^{2+}-depleted PS II sample, the Mn K-edge energy upshifted by 1 eV upon one-flash illumination that is a value typical of the S_1-to-S_2 transition. Thus, FTIR difference spectrum of this Ca^{2+}-depleted PS II membranes induced by single-pulse illumination (Fig. 2B) represents the S_2/S_1 spectrum as well as the case of untreated PS II membranes (Fig. 2A). Absence of the Q_A^-/Q_A [24] and Fe(II)/Fe(III) [22] signals again indicates no contribution of the acceptor-side changes to the spectrum. Both of the spectra (Figs. 2A and 2B) were normalized on the bases of CN stretching bands of ferricyanide (2115 cm^{-1}) and ferrocyanide (2037 cm^{-1}) (the region of these bands is not shown in Fig. 2), so that the two spectra in the figure represent the same amount of S_1-to-S_2 changes and direct comparison of these spectra becomes possible.

It is noted that the absolute intensity of the spectrum (see scale bars) is smaller by about factor of two in Ca^{2+}-depleted PS II than untreated PS II. This is because the temperature dependence of the S_2 formation shifts to higher temperatures by about 50°C for Ca^{2+}-depleted OEC

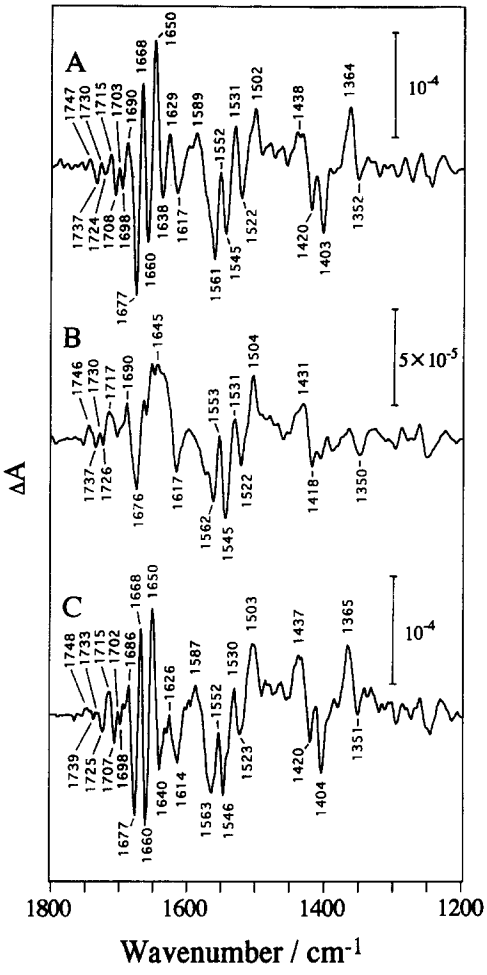

Fig. 2. Single-pulse induced S_2/S_1 FTIR difference spectra of untreated PS II membranes (identical to Fig. 1A) (A), Ca^{2+}-depleted PS II membranes (B), and Ca^{2+}-reconstituted PS II membranes (C). The three spectra were normalized on the ferrocyanide band at 2037 cm^{-1} (not shown). Ca^{2+} depletion was performed by low-pH treatment in the dark. The measurement conditions were the same as in Fig. 1A. The buffer for (B) included 0.5 mM EDTA instead of 20 mM $CaCl_2$ in the buffer for (A) and (C). Ten and five spectra with different samples were averaged for (B) and (C), respectively.

preserving the 24 and 16 kDa proteins compared with untreated OEC, and hence the efficiency of the S_2 formation at 250 K is about half of the untreated PS II [26]. Evidence that the signal decrease is not due to sample degradation was obtained in the Ca^{2+}-reconstitution experiment (see below). Also, absence of signals typical of other redox components on the donor side, i.e., a positive band at 1660 cm^{-1} for Cytochrome *b*-559 [28], a positive band at 1714 cm^{-1} and negative bands at 1684 and 1660 cm^{-1} for accessory chlorophyll (Noguchi et al., unpublished), positive bands at 1465, 1441, 1148, and 992 cm^{-1} for carotenoid (Noguchi et al., unpublished), indicates that the changes of these components do not take place in Ca^{2+}-depleted PS II by single-pulse illumination at 250 K.

Comparison between the untreated (Fig. 2A) and Ca^{2+}-depleted (Fig. 2B) S_2/S_1 spectra shows that Ca^{2+} deple-

tion induced dramatic changes in the regions of 1400–1350 cm^{-1} and in 1700–1600 cm^{-1}; upon Ca^{2+} depletion, the 1403 (−) and 1364 (+) cm^{-1} bands (hereafter, positive and negative bands are represented by + and −, respectively) were completely lost, and the complex structures in 1700–1600 cm^{-1} almost disappeared.

When the Ca^{2+}-depleted PS II membranes are supplemented with exogenous Ca^{2+} (Fig. 2C), these changes are largely restored, and the resulting spectrum is practically the same as that of untreated PS II (Fig. 2A). This means that the spectral changes caused by Ca^{2+} depletion are reversible and reflect only the effects of the loss of Ca^{2+}.

Fig. 3A shows the expanded view of the untreated (solid curve) and Ca^{2+}-depleted (dotted curve) S_2/S_1 spectra in the 1620–1300 cm^{-1} region. Normalization of the spectra was done on the large ferrocyanide band (2037 cm^{-1}) as the spectra in Fig. 2. The specific disappearances of the 1403 (−) and 1364 (+) cm^{-1} bands upon Ca^{2+} depletion were clearly seen in this superimposed view. Also, the 1561 cm^{-1} (−) band decreases its intensity and 1589 cm^{-1} (+) band almost disappears. Other bands were basically unchanged, although small intensity changes and frequency shifts were observed. The observation that no new band appeared upon Ca^{2+} depletion confirms that the S_2/S_1 spectrum in Ca^{2+}-depleted PS II membranes was correctly obtained and there was no contamination of other changes such as the S_2-to-S_3 transition and reactions of other redox components.

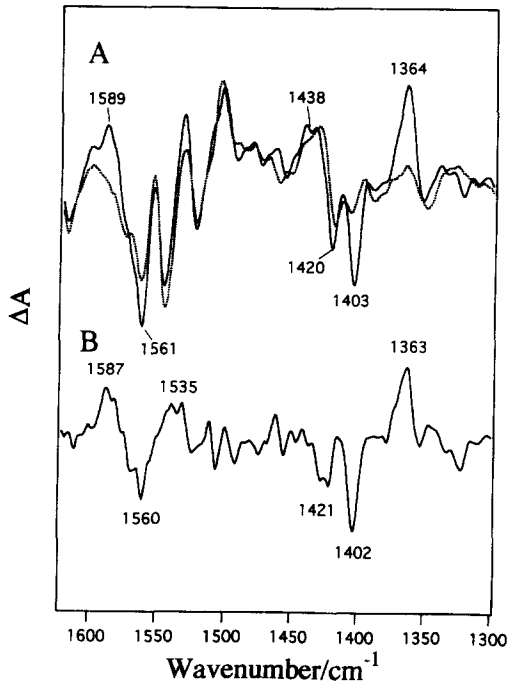

Fig. 3. (A) Expanded view (1620–1300 cm^{-1}) of the S_2/S_1 difference spectra of untreated (solid curve) and Ca^{2+}-depleted (dotted curve) PS II membranes. The two spectra were normalized on the ferrocyanide band at 2037 cm^{-1} (not shown). (B) Double difference spectrum calculated by subtraction of the Ca^{2+}-depleted spectrum (Fig. 3A dotted curve) from the untreated spectrum (Fig. 3A solid curve).

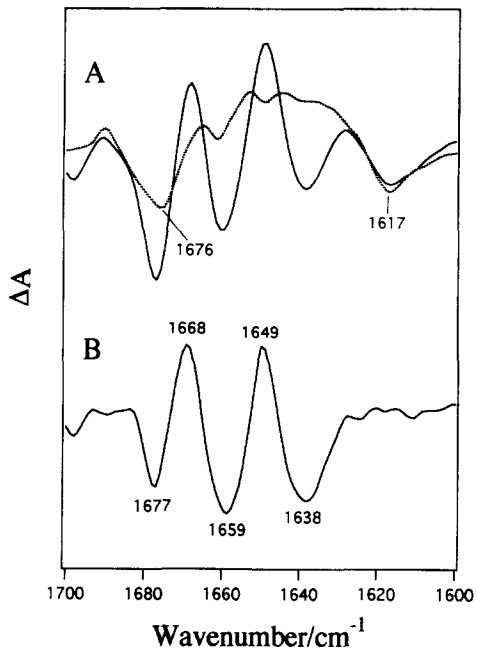

Fig. 4. (A) Expanded view (1700–1600 cm^{-1}) of the S_2/S_1 difference spectra of untreated (solid curve) and Ca^{2+}-depleted (dotted curve) PS II membranes. The two spectra were normalized on the ferrocyanide band at 2037 cm^{-1} (not shown). (B) Double difference spectrum calculated by subtraction of the Ca^{2+}-depleted spectrum (Fig. 4A dotted curve) from the untreated spectrum (Fig. 4A solid curve).

These spectral changes are more easily seen in the double difference spectrum (Fig. 3B) calculated by subtraction of the Ca^{2+}-depleted S_2/S_1 spectrum (Fig. 3A dotted curve) from the untreated one (Fig. 3A solid curve). Note that the subtraction was performed after normalization of the two spectra on the 2037 cm^{-1} ferrocyanide band. (All the double difference spectra hereafter were calculated in the same way.) The bands at 1402 (−), 1363 (+), 1560 (−) and 1587 (+) cm^{-1} were clearly seen corresponding to the band disappearances or intensity decrease mentioned above. Other than these bands, a negative band at 1421 cm^{-1} and a positive band at 1535 cm^{-1} were observed, among which the former clearly results from slight shifts and intensity changes of the 1438/1420 cm^{-1} bands.

Fig. 4A shows the expanded view of the untreated (solid curve) and Ca^{2+}-depleted (dotted curve) S_2/S_1 difference spectra in the 1700–1600 cm^{-1} region, which were normalized on the ferrocyanide band. Upon Ca^{2+}-depletion, most of the strong differential bands were lost altogether, while the bands at 1676 (−) and 1617 (−) cm^{-1} were left in the spectrum. The broad positive band around 1645 cm^{-1} were also left after Ca^{2+} depletion, although some artifact due to subtraction of the large amide I absorption (about 10^4-times larger than the scale of the difference spectra in Fig. 4) might contribute to the part of this band because of the somewhat unnatural band shape.

Fig. 4B shows a double difference spectrum between the above two spectra (solid curve minus dotted curve). It was clearly demonstrated that the bands at 1677 (−), 1668 (+), 1659 (−), 1649 (+) and 1638 (−) cm^{-1} were lost upon Ca^{2+} depletion.

3.3. S_2/S_1 spectra of ^{15}N-labeled PS II membranes

In order to investigate the contribution of nitrogen atoms to the vibrational modes in the S_2/S_1 spectra, spectra of ^{15}N-labeled PS II membranes were measured. Fig. 5 shows the S_2/S_1 spectra of ^{15}N-labeled PS II membranes (solid curve) together with that of natural (^{14}N) PS II membranes (dotted curve). These two spectra were normalized on the ferrocynide band at 2037 cm^{-1} (the region not shown). The most drastic changes were observed in the 1500–1550 cm^{-1} region; the structures with peaks at 1545 (−), 1531 (+), and 1522 (−) cm^{-1} were replaced by the 1539 (+) and 1529 (−) cm^{-1} bands in the ^{15}N-spectrum. Also, in the 1700–1600 cm^{-1} region, some intensity changes were observed, although there were no large shifts of peak positions. In the frequency region lower than 1450 cm^{-1}, practically no change was observed upon ^{15}N substitution. In particular, the 1403 (−) and 1364 (+) cm^{-1} bands, which disappeared upon Ca^{2+} depletion (Fig. 3), was not affected at all by ^{15}N substitution both in their positions and intensities, indicating that these vibrational modes were unrelated to nitrogen atoms.

Fig. 6A shows Ca^{2+}-depleted (solid curve) and untreated (dotted curve, identical to Fig. 5 solid curve) S_2/S_1 difference spectra of ^{15}N-labeled PS II membranes. Again, the two spectra were normalized on the ferrocyanide band. A double difference spectrum between these spectra (dotted curve minus solid curve) are shown in Fig. 6B. This double difference spectrum of ^{15}N-labeled PS II membranes corresponds to the natural (^{14}N) ones in Figs. 3B and 4B. The prominent change upon ^{15}N substitution in the untreated-minus-Ca^{2+}-depleted S_2/S_1 spectrum is that new differential bands at 1522 (−) and 1512 (+) cm^{-1} appeared instead of the 1535 (+) band (Fig. 3B). Also, the 1560 (−) cm^{-1} peak (Fig. 3B) seems to slightly shift to a higher frequency of 1564 cm^{-1}. These changes can be interpreted that the band at 1535 (+) cm^{-1} and some contribution of the 1560 (−) cm^{-1} band downshifted upon ^{15}N substitution, and the new 1512 (+) and 1522 (−) cm^{-1} bands appeared. This indicates that these bands are ascribed to the modes including nitrogen atoms. On the other hand, the remaining bands at 1586 (+) and 1564 (−) cm^{-1} is considered to be due to the modes unrelated to nitrogen atoms.

In the 1700–1600 cm^{-1} region, the several intense bands that disappeared upon Ca^{2+} depletion were not basically influenced by ^{15}N-substitution; The 1678 (−), 1670 (+), 1658 (−), 1650 (+), and 1639 (−) bands in Fig. 6B (^{15}N-labeled PS II) correspond to the 1677 (−), 1668 (+), 1659 (−), 1649 (+), and 1638 (−) bands in Fig. 4B (natural PS II).

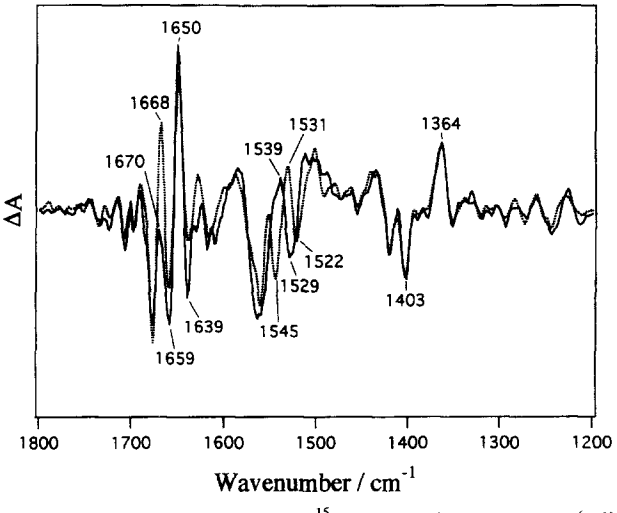

Fig. 5. S_2/S_1 difference spectrum of ^{15}N-labeled PS II membranes (solid curve) compared with that of natural (^{14}N) PS II membranes (dotted curve, identical to Fig. 1A). The measurement conditions were the same as in Fig. 1A. Five spectra with different samples were averaged. The two spectra were normalized on the ferrocyanide band at 2037 cm^{-1}.

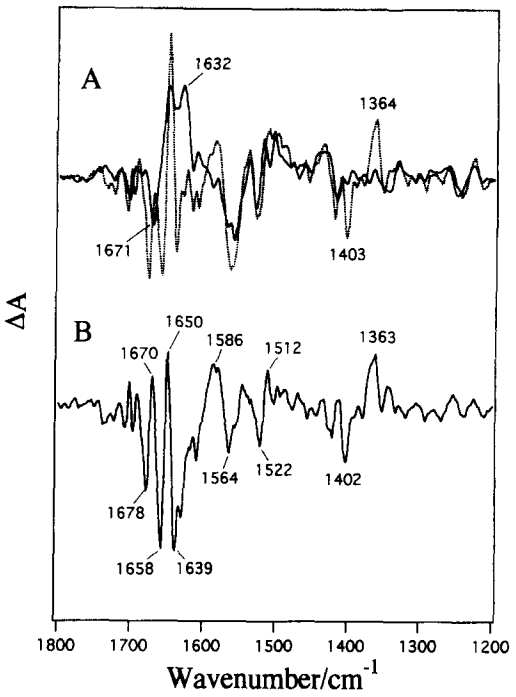

Fig. 6. (A) S_2/S_1 difference spectrum of ^{15}N-labeled Ca^{2+}-depleted PS II membranes (solid curve) compared with that of ^{15}N-labeled untreated PS II membranes (dotted curve, identical to the Fig. 5 solid curve). The used buffer and measurement conditions were the same as those for Fig. 2B. Ten spectra with different samples were averaged. The two spectra were normalized on the ferrocyanide band at 2037 cm^{-1}. (B) Double difference spectrum calculated by subtraction of the ^{15}N-labeled Ca^{2+}-depleted spectrum (Fig. 6A solid curve) from the ^{15}N-labeled untreated spectrum (Fig. 6A dotted curve).

4. Discussion

The single-pulse induced FTIR difference spectra of PS II membranes measured in this study reflect structural changes in OEC upon S_1-to-S_2 transition. The spectra consist of only the signals from OEC and do not include acceptor-side signals, because an electron was abstracted from PS II by ferricyanide that does not have bands in the 1800–1000 region, and the redox reactions of the non-heme iron was restrained by controlling the redox potential and pH of the buffer. The S_2/S_1 spectra thus obtained was practically the same as the double difference spectrum between the $S_2Q_A^-/S_1Q_A$ and Q_A^-/Q_A spectra measured with continuous illumination, confirming the idea that all the bands in the flash-induced spectra in 1800–1000 cm^{-1} are ascribed to the S_1-to-S_2 changes. In these difference spectra, bands with negative and positive intensities belong to the S_1 and S_2 states, respectively.

Generally, IR spectra can be interpreted by the idea of characteristic group frequencies; functional groups in a given substance show characteristic absorption bands and the correlations between them have been derived from numerous data collected over many years (For general tables and charts of infrared group frequencies, see [29]). For proteins, backbone amide groups (-CONH-) and functional groups in amino-acid side chains, i.e., $-CH_3$ and $-CH_2-$ in most of amino acids, $-COO^-$ or -COOH in Asp, Glu and C-terminus, $-CONH_2$ in Asn and Gln, $-NH_3^+$ in Lys and N-terminus, -OH in Ser, Thr and Tyr, -SH in Cys, -S- in Met, guanidine ($CN_3H_5^+$) in Arg, imidazole in His, phenyl group in Phe, phenol in Tyr, and indole in Trp, should be considered. Although OEC includes metals (Mn and Ca), vibrational modes related to metals usually show bands at frequencies lower than 1000 cm^{-1} [29], and hence in the 1800–1000 cm^{-1} region measured in the present study, the metal vibrations are not necessary to be considered. Water has only one band near 1645 cm^{-1} in this region due to H–O–H bending mode, but D_2O-exchange experiments showed that the contribution of this mode to the S_2/S_1 difference spectrum is small enough (Noguchi et al., unpublished data).

Venyaminov and Kalnin [30,31] investigated IR spectra of all 20 amino acids and proteins in water and provided the assignments and extinction coefficients of the bands in 1800–1480 cm^{-1}. (The extinction coefficients of the prominent bands were given even in the region lower than 1480 cm^{-1}.) We also measured FTIR spectra of 20 amino acids both in water and 1 M HCl solution (for Tyr, only in HCl solution) in order to supplement the data by Venyaminov and Kalnin [30] especially in the region lower than 1500 cm^{-1} (data not shown). Amino acids in 1 M HCl solutions were measured for detecting the bands near 1400 cm^{-1}, where an intense symmetric COO^- stretching band of and α-carboxyl group overlaps in H_2O but absent in 1 M HCl solution due to protonation of this group. Extinction coefficients of the bands in the region lower than 1500 cm^{-1} was estimated on the basis of those of the known bands in the 1800–1500 cm^{-1} region determined by Venyaminov and Kalnin [30].

4.1. Assignments of the symmetric COO^- stretching bands

As shown in Fig. 3, upon Ca^{2+} depletion, an intense negative band at 1403 cm^{-1} and a positive band at 1364 cm^{-1} in the S_2/S_1 difference spectrum clearly disappeared. The most intense (large in the extinction coefficient) IR bands in the 1450–1350 cm^{-1} region in proteins are symmetric COO^- stretching bands of Asp, Glu, and C-terminus (α-COO^-) (ϵ = 200–320 L mol^{-1} cm^{-1} [30]). Although these bands are located in 1412–1402 cm^{-1} as amino-acid solutions [30], it has been known that the positions of symmetric COO^- stretching bands considerably change within 1450–1300 cm^{-1} in metal complexes depending on the coordination structures [32,33]. Other possible bands in this region with medium intensities are the $-CH_2-$ scissoring band (1480–1440 cm^{-1}), the $-CH_3$ asymmetric (1465–1440 cm^{-1}) and symmetric (1390–1370 cm^{-1}) deformations, the C–N stretch of $-CONH_2$ (1420–1400), the O–H deformation of primary and secondary alcohols (1350–1260 cm^{-1}), the O–H deformation of -COOH (1380–1280 cm^{-1}), and the indole ring bands near 1460, 1420 and 1350 cm^{-1} [29].

In our measurements of all 20 amino acids in 1 M HCl solution, intensities of the observed bands in the 1450–1350 cm^{-1} region, which are the results of severe overlap of the various bands mentioned above other than the COO^-

Table 1
FTIR bands sensitive to Ca^{2+} depletion in the S_2/S_1 difference spectrum

Unlabeled PS II (positive/negative bands (cm^{-1}))	^{15}N-labeled PS II	Assignment
1668/1677	1670/1678	amide I (turns)
1668/1659	1670/1658	amide I (turns, random coil)
1649/1659	1650/1658	amide I (α-helix, random coil)
1649/1638	1650/1639	amide I (β-strands)
1587/1560	1586/1564	asymmetric COO^- stretch
1535/1560	1512/1522	amide II
1364/1403	1364/1403	symmetric COO^- stretch

stretch (-COO^- does not exist in 1 M HCl), were at most 30% of the C = O stretching band of α-COOH at about 1740 cm^{-1} (ϵ = 170 L mol^{-1} cm^{-1} [30]). This means that the extinction coefficient of each band is less than 50 L mol^{-1} cm^{-1}, which is much smaller than the symmetric COO^- bands (ϵ = 200–320 L mol^{-1} cm^{-1} [30]). Also, the results of measurements indicate that, even if there are complex vibrations that cannot be interpreted by simple group frequencies, intensities of such bands will be as small as the above bands.

Since the 1403 (−) and 1364 (+) bands appeared as considerably strong bands in the 1800–1000 cm^{-1} region of the S_2/S_1 difference spectrum (Fig. 1A), the primary candidate for the assignments of these bands is of course the symmetric COO^- stretching mode, which has the strongest intensity in the 1450–1350 cm^{-1} region. The result that these two bands were not affected at all by ^{15}N substitution (Fig. 5, Table I), supports these assignments and also completely excludes the possibilities of the C–N stretching vibration of -$CONH_2$ groups and any nitrogen-relating vibrations. The -CH_2- scissor and -CH_3 deformations are also not possible, because these vibrations are not sensitive to molecular interactions and environmental changes, and a large frequency shift such as from 1403 to 1364 cm^{-1} cannot occur as long as drastic chemical reactions do not take place. Furthermore, the possibility of O–H deformations of alcohols and carboxylic acids are unlikely, because the C–O (1200–1000 cm^{-1} in alcohols and 1300–1100 cm^{-1} in carboxylic acids) or C = O (1750–1700 cm^{-1} in carboxylic acids) stretching bands of these groups should have much stronger intensities than the O–H deformation bands [29], but no such bands with intensities comparable to the 1403 and 1364 cm^{-1} bands were found in the regions of these vibrations (Fig. 1A).

As a conclusion, the intense 1403 (−) and 1364 (+) bands can be assigned to the symmetric COO^- stretching modes. Although we think that the above considerations are enough to assign these bands correctly, it is noted that specific isotope labeling of Asp and Glu side chains will provide final direct evidence for these assignments.

The observation that no bands as strong as the 1403 and 1364 cm^{-1} ones appeared in the C = O stretching region of -COOH groups (1750–1700 cm^{-1}) (Fig. 1A) indicates that neither protonation nor deprotonation reactions of the -COO^- and -COOH groups are related to the appearances of the 1403 and 1364 cm^{-1} bands. This is consistent with the previous observation by Rappaport and Lavergne [34] that in PS II membranes almost no proton release takes place upon S_1-to-S_2 transition at pH 5.5. When a certain COO^- group is perturbed in some way without a protonation reaction, a difference spectrum should exhibit a set of negative (before perturbation) and positive (after perturbation) bands within the symmetric COO^- region (1450–1300 cm^{-1}). Since the 1403 (−) and 1364 (+) cm^{-1} bands were lost together upon Ca^{2+} depletion, and these were the only bands influenced in this region, it can be concluded that these negative and positive bands come from an identical carboxylate group in the S_1 and S_2 states, respectively.

4.2. Assignments of the asymmetric COO^- stretching bands

A carboxylate group exhibits one more absorption band, an asymmetric COO^- stretching band, coupled with the symmetric one [32,33]. As for amino acids in water, carboxylate groups in the side chains of Asp and Glu show this band at 1574 and 1560 cm^{-1}, respectively, and an α-carboxylate group (corresponding to the C-termini) shows the band at 1598 cm^{-1} [30]. As the case of the symmetric band, this asymmetric one is sensitive to molecular interactions and coordination structures and the band positions change depending on these natures [32,33]. Also, asymmetric COO^- bands have intensities comparable to or even stronger than the symmetric ones (ϵ = 200–500 L mol^{-1} cm^{-1} in amino acids in water [30]). Therefore, in the S_2/S_1 spectra there should be contributions of the asymmetric COO^- bands coupled with the symmetric ones at 1403 (−) and 1364 (+) cm^{-1}, and these asymmetric bands should be lost upon Ca^{2+} depletion accompanied by the loss of the symmetric ones.

Although band changes near 1550 cm^{-1} upon Ca^{2+} depletion were not as simple as the changes near 1400 cm^{-1} (Fig. 3A), the double difference spectrum (Fig. 3B) between the untreated and Ca^{2+}-depleted S_2/S_1 spectra clearly showed that the bands at 1587 (+), 1560 (−) and 1535 (+) cm^{-1} were lost upon Ca^{2+} depletion. Furthermore, it was shown that upon ^{15}N substitution, the positive 1535 cm^{-1} band and probably the part of the negative 1560 cm^{-1} band shifted to the lower frequencies at 1512 (+) and 1522 (−) cm^{-1}, while the 1587 (+) and 1560 (−) cm^{-1} bands were basically left to be unchanged (Fig. 6B, Table I). (A slight upshift of the 1560 (−) cm^{-1} band to 1564 (−) cm^{-1} may be due to the downshift of the band partly overlapping at 1560 cm^{-1}.)

Possible vibrational modes near 1550 cm^{-1} other than the asymmetric COO^- stretch are the amide II modes of backbone amide groups (N–H bending mode coupled with C–N stretch) (ϵ = 200–350 L mol^{-1} cm^{-1}) and the symmetric NH_3^+ deformation modes of Lys and the N-terminus (ϵ = 100--200 L mol^{-1} cm^{-1}) [30,31]. Since both the modes include nitrogen atoms and should be influenced by ^{15}N substitution, these modes are excluded from the assignments of the bands at 1587 (+) and 1560 (−) cm^{-1} unrelated to nitrogen vibrations. As a consequence, these bands can be assigned to the asymmetric COO^- stretching modes. It is noted that the bands that downshifted upon ^{15}N substitution (the positive band at 1535 cm^{-1} and a part of the negative band at 1560 cm^{-1} (Fig. 3B)) are most probably assigned to the amide II modes, because there is no N-termini and only one Lys residue is present on the lumenal side of the D1 and D2 proteins, where OEC is

thought to be located [3]. Thus, it can be concluded that the asymmetric COO^- stretching bands at 1560 (−) and 1587 (+) cm^{-1} are the counterparts of the symmetric bands at 1403 (−) and 1364 (+) cm^{-1}, respectively.

4.3. Coordination structure of the COO^- group and its changes

The asymmetric and symmetric COO^- stretching modes are coupled with each other, and the extent of coupling, which is affected by the coordination structures of the carboxylate group, decides the frequencies of these bands. Correlations between COO^- stretching frequencies and coordination structures have been extensively studied by using a number of carboxylate metal complexes [32,33]. Also, in some Ca^{2+}-binding proteins such as calmodulin and pike parvalbumin, the COO^- stretching bands have been used to investigate the interactions of amino-acid COO^- groups with metals and their coordination structures [35–37]. General criteria for determining the coordination structure from the frequency difference ($\Delta\nu$) between the asymmetric and symmetric modes have been proposed [32,33]; (i) In unidentate coordination, $\Delta\nu$ is greater ($> \approx 200$ cm^{-1}) than the free ionic value (≈ 160 cm^{-1}). (ii) A bridging bidentate structure exhibits a $\Delta\nu$ value close to the free ionic value (≈ 160 cm^{-1}). (iii) A significantly low $\Delta\nu$ value ($< \approx 100$ cm^{-1}) indicates chelating bidentate coordination.

The assignments of the COO^- bands described above indicated that a certain carboxylate group in OEC has its asymmetric and symmetric stretching bands at 1560 and 1403 cm^{-1}, respectively, in the S_1 state, and at 1587 and 1364 cm^{-1}, respectively, in the S_2 state. Thus, the $\Delta\nu$ values are 157 and 223 cm^{-1} in the S_1 and S_2 states, respectively. By employing the above criteria, we can conclude that the COO^- group responsible for these bands has a bridging bidentate structure in the S_1 state, but has a unidentate structure in the S_2 state.

It should be noted that the same conclusion can be obtained even when only the explicit band changes of the symmetric COO^- modes (1403 to 1364 cm^{-1}) are considered. According to Deacon and Phillips [32], bridging bidentate coordination shows COO^- stretching frequencies similar to the free ionic values, because of the equivalence of the two C − O bond orders. The unidentate coordination, however, removes this equivalence and hence coupling between the two C–O bonds is weakened, resulting in a decrease in the symmetric frequency and an increase in the asymmetric frequency [32]. The symmetric COO^- frequency of 1403 cm^{-1} in the S_1 state is close to the ionic values of acetate (1414 cm^{-1} [33]), β-COO^- of Asp (1402 cm^{-1}), γ-COO^- of Glu (1404 cm^{-1}), and α-COO^- (1412 cm^{-1}) [30], being indicative of a bridging bidentate structure. The large frequency decrease from 1403 to 1364 cm^{-1} upon S_2 formation indicates the coordination change of this COO^- group from a bridging to unidentate structure. Indeed, among the data of more than 70 acetate complexes collected by Deacon and Phillips [32] and Nakamoto [33], all the compounds that exhibit symmetric COO^- bands lower than 1380 cm^{-1} take unidentate coordination, with a few exceptions whose data were claimed to be incorrect [32].

Since the above COO^- changes are induced by single-electron oxidation of the Mn-cluster through the S_1-to-S_2 transition, this COO^- group most probably ligates to at least one of the redox-active Mn ions. Also, the fact that

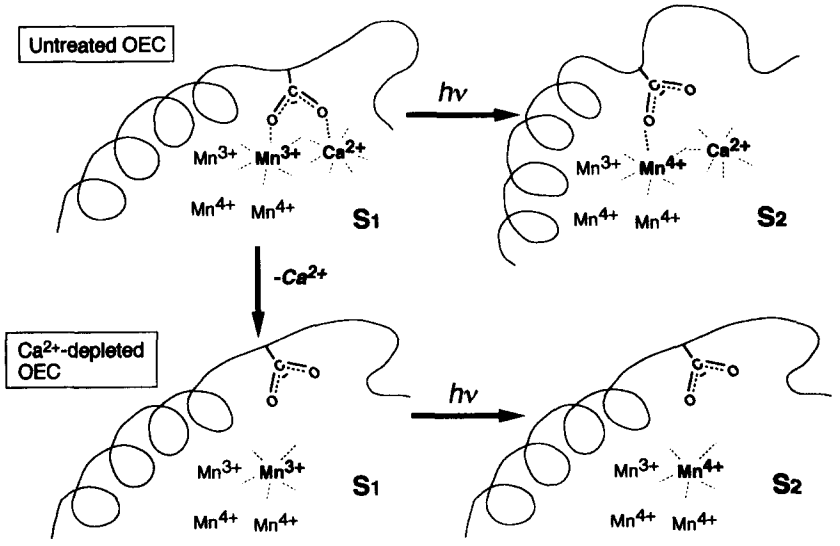

Fig. 7. Schematic picture of the structural changes of OEC with regard to Ca^{2+}. Protein moieties around the Mn-cluster are represented by a single polypeptide chain for simplicity. A carboxylate group of the protein serves as a bridging ligand between the redox-active Mn and Ca^{2+} ions in the S_1 state. Upon S_2 formation, the coordination bond to Ca^{2+} is selectively broken, accompanied with some conformational changes of the protein around the Mn-cluster. Upon Ca^{2+} depletion, this carboxylate is liberated from the Mn-cluster and the light-induced conformational changes no longer take place.

these COO^- bands specifically disappear upon Ca^{2+} depletion, implies close structural relevance of this COO^- group to Ca^{2+}. The most plausible view is that this COO^- group simultaneously ligates to the Mn and Ca^{2+} ions in the S_1 state. Another possibility that this group ligates to the two Mn ions can be excluded by taking into consideration the following facts: (i) one of the coordination bonds of this COO^- group should be broken upon S_2 formation, because this group takes an unidentate structure in the S_2 state, but (ii) no large rearrangement in the ligand atoms of the Mn ions was observed between the S_1 and S_2 states in the extended X-ray absorption fine structure (EXAFS) studies [4], namely, breakage of the coordination bond of this COO^- to Mn upon S_2 formation is likely to occur. Thus, it is concluded that this COO^- group coordinates to Mn and Ca^{2+} to form a bridging structure in the S_1 state. The above consideration further leads to a conclusion that, of these two coordination bonds, the bond to Ca^{2+} is selectively broken upon S_2 formation and the COO^- group becomes unidentate coordination.

Since no new band was generated in Ca^{2+}-depleted PS II in place of the lost 1587/1560 and 1364/1403 cm^{-1} bands, it is considered that this COO^- group is liberated even from the Mn ion upon Ca^{2+} depletion. The resultant free COO^- group may be barely affected by oxidation of the Mn-cluster, and the bands of this group will not be observed in the difference spectrum upon S_2 formation. This conclusion is consistent with the results of XANES study on Ca^{2+}-depleted PS II [38], in which the decrease in K-edge energy by about 1 eV upon Ca^{2+} depletion has been interpreted as breakage of the coordination bond of a ligand of the Mn-cluster. These coordination changes of the bridging carboxylate are schematically depicted in Fig. 7.

The presence of a carboxylate bridge between Mn and Ca^{2+} and the dynamic changes of its coordination structure upon S_2 formation and Ca^{2+} depletion may consistently explain various experimental findings so far reported; (i) The low-pH treatment for Ca^{2+} depletion [39] agrees with the presence of carboxylate ligands of Ca^{2+}. (ii) The carboxylate bridge between Mn and Ca^{2+} is consistent with the close vicinity of Ca^{2+} from the Mn-cluster predicted by EXAFS and EPR studies [10,11,13,14]. (iii) The breakage of the coordination bond to Ca^{2+} upon S_2 formation explains why Ca^{2+} removal by NaCl-treatment is more facilitated in higher S-states [40]. (iv) The liberation of a carboxylate ligand from the Mn-cluster by Ca^{2+} depletion explains the enhanced accessibility of reductants such as NH_2OH [41,42] and of chelators [43] to the Mn-cluster in Ca^{2+}-depleted PS II.

The amino-acid residue responsible for the carboxylate bridge between Mn and Ca^{2+} is most probably provided by Asp, Glu or the C-terminus residing on the lumenal side of the D1 or D2 polypeptides. All the conserved amino-acid residues with a carboxylate group in the lumenal regions of the D1 and D2 polypeptides were genetically changed (reviewed in [3]). The resultant mutants at Glu-70 of D2, and Asp-59, Asp-61, Glu-65, Asp-170, Glu-189, Glu-333, Asp-342 and the C-terminus (Ala-344) of D1 impaired the capability of photoautotrophic growth, and hence all these residues can be candidates for the bridging ligand. Although it is difficult to definitely identify the amino-acid residue of this bridging ligand at the present stage, further FTIR spectroscopic studies assisted by mutagenesis will provide a clear answer to this question.

4.4. Conformational changes of the protein around the Mn-cluster

Along with the disappearance of the COO^- bands, several intense bands in 1680–1630 cm^{-1}, i.e., the 1677 (−), 1668 (+), 1659 (−), 1649 (+), and 1638 (−) cm^{-1} bands, were lost upon Ca^{2+} depletion (Fig. 4). In this region, the most prominent vibrational bands in proteins are the amide I bands (C = O stretches of the amide groups) of backbone chains (1700–1600 cm^{-1}, ϵ = 300–1000 L mol^{-1} cm^{-1} [31]). Other modes possible for the bands in 1680–1630 cm^{-1} are the C = O stretching (1680–1670 cm^{-1}, ϵ = 300–400 L mol^{-1} cm^{-1}) modes of $-CONH_2$ groups in Asn and Gln, the asymmetric stretching mode of the guanidine group ($-CN_3H_5^+$) ($\approx$ 1673 cm^{-1}, ϵ = 420 L mol^{-1} cm^{-1}) and its symmetric mode ($\approx$ 1633 cm^{-1}, ϵ = 300 L mol^{-1} cm^{-1}) in Arg, the symmetric NH_3^+ deformation mode in Lys and N-terminus (α-NH_3^+) ($\approx$ 1630 cm^{-1}, ϵ = 100–250 L mol^{-1} cm^{-1}) [30].

Since the positions of the bands lost upon Ca^{2+} depletion in 1680–1630 cm^{-1} were basically unchanged upon ^{15}N substitution (Fig. 6B), possibilities of the stretching modes of guanidine groups and deformation modes of $-NH_3^+$ groups out of the above modes can be excluded for the assignments of these bands. Although we cannot entirely exclude the possibility of the C = O stretching mode of $-CONH_2$ groups, the fact that the NH_2 deformation mode of $-CONH_2$ groups (1625–1610 cm^{-1}, ϵ = 150–250 L mol^{-1} cm^{-1} [30]) was not found in the bands lost upon Ca^{2+} depletion (this band should largely downshift by ^{15}N substitution), makes the assignment to the $-CONH_2$ vibrations unlikely. As a consequence, the intense bands in 1680–1630 cm^{-1} are assignable to the amide I modes of protein backbones. These assignments are quite reasonable, because amide I bands are known to be sensitive to subtle changes of the protein conformations [44], and corresponding changes of the amide II bands were also observed near 1550 cm^{-1} (see above). It should be noted that although the bands thus assigned to the amide I modes, which is weakly coupled with C–N stretching and N–H bending modes [45], were practically unaffected by ^{15}N substitution (Figs. 4B and 6B, Table I), the ^{15}N-induced shift of the amide I peak in the original (not difference) spectrum of PS II membranes was also only 1 cm^{-1} from 1658 to 1657 cm^{-1}.

The above assignments of the amide I bands imply that the structures of protein backbones around the Mn-cluster are perturbed upon S_2 formation, and further, these structural changes require the presence of Ca^{2+} in OEC. These perturbations are probably relatively small structural changes within each conformation, because the observed band intensities are not significantly large as compared with those of other C = O bands. We also note that an amide I mode is coupled with numerous amide C = O bonds in polypeptide chains, so that the perturbation either on a particular amide C = O or on an overall chain can cause a frequency change.

Amide I bands can be generally assigned to each secondary structures by use of the criteria in literatures [44,46]. Since these criteria are mostly based on D_2O measurements, we must take into consideration that the band positions in H_2O are higher by 5–10 cm^{-1} than those in D_2O [44,46]. Because the bands in the amide I region of Fig. 4 severely overlap each other, we will take a middle position of the neighboring negative and positive peaks as the position of the amide I bands. The bands around 1673 cm^{-1} (1668/1677 cm^{-1}) are assigned to turns, those around 1664 cm^{-1} (1668/1659 cm^{-1}) to turns or random coil structures, those around 1654 cm^{-1} (1649/1659 cm^{-1}) to α-helical or random coil structures, and those around 1644 cm^{-1} (1649/1638 cm^{-1}) to β-strands (Table I). These assignments imply that there are several types of conformational structure around the Mn-cluster being influenced by S_2 formation. This agrees with the view that the OEC resides in the lumenal domain of the D1 and D2 polypeptides protruding out of the membrane [3].

The above conformational changes upon S_2 formation are not simply resulted from charge accumulation on the Mn-cluster, because Ca^{2+}-depleted OEC can accumulate a positive charge in its S_2 state like the normal S_2 state, but shows no conformational changes. The possible view is that the conformational changes are triggered by the coordination change of the bridging carboxylate connecting the Mn-cluster and Ca^{2+}. The Ca^{2+}-dependent conformational changes are depicted in Fig. 7, as represented by a single polypeptide chain for simplicity.

4.5. Roles of Ca^{2+} in the oxygen-evolving reactions

From the findings obtained in the present FTIR study, roles of Ca^{2+} in the oxygen-evolving reactions are argued as follows; (i) Ca^{2+} is necessary to stabilize the OEC structure in an active form. Ca^{2+} is connected with the Mn-cluster via a carboxylate bridge, and upon Ca^{2+} depletion, this carboxylate ligand is liberated from the Mn ion to alter the ligand structure of the Mn-cluster. This altered Mn-cluster no more exhibits the conformational changes upon S_2 formation, which may be needed for subsequent reaction steps (see below). (ii) The carboxylate group, which connects both Mn and Ca^{2+} in the S_1 state and becomes unidentate in the S_2 state by breakage of the coordination to Ca^{2+}, may work as a molecular pump to take out protons from the water molecules bound to the Mn-cluster. Indeed, an optical absorption study has proposed that deprotonation of water is blocked in Ca^{2+}-depleted PS II [47]. (iii) The conformational changes of proteins around the Mn-cluster upon the S_2 formation, which requires the presence of Ca^{2+}, may provide a reaction field necessary for water cleavage and a proton pathway in the proteins.

Acknowledgements

We would like to thank Dr. M. Nara for useful discussion and sending a preprint of his work. This work was supported by a grant for Photosynthetic Sciences and a Special Grant for Promotion of Research (to T.N.) at The Institute of Physical and Chemical Research (RIKEN) given by the Science and Technology Agency (STA) of Japan, and partially by grants from a Grant-in-Aid for Cooperative Research (No.05305004 and 05304006) and for Scientific Research on Priority Area (No. 05266221) (to T.O.) from the Ministry of Education, Science and Culture of Japan.

References

[1] Joliot, P., Barbieri, G. and Chabaud, R. (1969) Photochem. Photobiol. 10, 309–329.
[2] Kok, B., Forbush, B. and McGloin, M. (1970) Photochem. Photobiol. 11, 457–475.
[3] Debus, R.J. (1992) Biochim. Biophys. Acta 1102, 269–352.
[4] Sauer, K., Yachandra, V.K., Britt, R.D. and Klein, M.P. (1992) in Manganese Redox Enzymes (Pecoraro, V.L., ed.), pp. 141–175, VCH Publishers, New York.
[5] DeRose, V.J., Yachandra, V.K., McDermott, A.E., Britt, R.D., Sauer, K. and Klein, M.P. (1991) Biochemistry 30, 1335–1341.
[6] Tang, X.-S., Diner, B.A., Larsen, B.S., Gilchrist, M.L., Lorigan, G.A. and Britt, R.D. (1994) Proc. Natl. Acad. Sci. USA 91, 704–708.
[7] Tang, X.-S., Sivaraja, M. and Dismukes, G.C. (1993) J. Am. Chem. Soc. 115, 2382–2389.
[8] Yocum, C.F. (1991) Biochim. Biophys. Acta 1059, 1–15.
[9] Ono, T. and Inoue, Y. (1989) Biochim. Biophys. Acta 973, 443–449.
[10] Ono, T. and Inoue, Y. (1989) Arch. Biochem. Biophys. 275, 440–448.
[11] Boussac, A. and Rutherford, A.W. (1988) Biochemistry 27, 3476–3483.
[12] Boussac, A., Zimmermann, J-L. and Rutherford, A.W. (1989) Biochemistry 28, 8984–8989.
[13] Penner-Hahn, J.E., Fronko, R.M., Pecoraro, V.L., Yocum, C.F., Betts, S.D. and Bowlby, N.R. (1990) J. Am. Chem. Soc. 112, 2549–2557.
[14] Yachandra, V.K., DeRose, V.J., Latimer, M.J., Mukerji, I., Sauer, K. and Klein, M.P. (1993) Science 260, 675–679.
[15] Noguchi, T., Ono, T. and Inoue, Y. (1992) Biochemistry 31, 5953–5956.
[16] Noguchi, T., Ono, T. and Inoue, Y. (1992) in Research in Photosynthesis (Murata, N., ed.), Vol.II, pp. 309–312, Kluwer, Dordrecht.
[17] Noguchi, T., Ono, T. and Inoue, Y. (1993) Biochim. Biophys. Acta 1143, 333–336.

[18] Berthold, D.A., Babcock, G.T. and Yocum, C.F. (1981) FEBS Lett. 134, 231–234.
[19] Ono, T. and Inoue, Y. (1986) Biochim. Biophys. Acta 850, 380–389.
[20] Ono, T., Izawa, S. and Inoue, Y. (1992) Biochemistry 31, 7648–7655.
[21] Petrouleas, V. and Diner, B.A. (1986) Biochim. Biophys. Acta 849, 264–275.
[22] Hienerwadel, R., Boussac, A. and Berthomieu, C. (1993) in Fifth International Conference on the Spectroscopy of Biological Molecules (Theophanides, T., Anastassopoulou, J. and Fotopoulos, N., eds.), pp. 317–318, Kluwer, Dordrecht.
[23] Vass, I. and Styring, S. (1991) Biochemistry 30, 830–839.
[24] Berthomieu, C., Nabedryk, E., Mäntele, W. and Breton, J. (1990) FEBS Lett. 269, 363–367.
[25] Renger, G., Hagemann, R. and Dohnt, G. (1981) Biochim. Biophys. Acta 636, 17–26.
[26] Ono, T. and Inoue, Y. (1990) Biochim. Biophys. Acta 1015, 373–377.
[27] Ono, T., Noguchi, T., Inoue, Y., Kusunoki, M., Yamaguchi, H. and Oyanagi, H. (1993) FEBS Lett. 330, 28–30.
[28] Berthomieu, C., Boussac, A., Mäntele, W., Breton, J. and Nabedryk, E. (1992) Biochemistry 31, 11460–11471.
[29] Socrates, G. (1994) Infrared Characteristic Group Frequencies, 2nd Edn., Wiley, Chichester.
[30] Venyaminov, S. Yu. and Kalnin, N.N. (1990) Biopolymers 30, 1243–1257.
[31] Venyaminov, S. Yu. and Kalnin, N.N. (1990) Biopolymers 30, 1259–1271.
[32] Deacon, G.B. and Phillips, R.J. (1980) Coord. Chem. Rev. 33, 227–250.
[33] Nakamoto, K. (1986) Infrared and Raman Spectra of Inorganic and Coodination Compounds, pp. 231–233, Wiley, New York.
[34] Rappaport, F. and Lavergne, J. (1991) Biochemistry 30, 10004–10012.
[35] Nara, M., Tanokura, M. and Tasumi, M. (1993) in Proceedings of the 9th International Conference on Fourier Transform Spectroscopy (Bertie, J.E. and Wieser, H., eds.), Vol. 2089, pp. 344–345, the Society of Photo-Optical Instrumentation Engineers, Washington.
[36] Nara, M., Tasumi, M., Tanokura, M., Hiraoki, T., Yazawa, M. and Tsutsumi, A. (1994) FEBS Lett. 349, 84–88.
[37] Tasumi, M. (1993) in Fifth International Conference on the Spectroscopy of Biological Molecules (Theophanides, T., Anastassopoulou, J. and Fotopoulos, N., eds.), pp. 173–176, Kluwer, Dordrecht.
[38] Ono, T., Kusunoki, M., Matsushita, T., Oyanagi, H. and Inoue, Y. (1991) Biochemistry 30, 6836–6841.
[39] Ono, T. and Inoue, Y. (1988) FEBS Lett. 227, 147–152.
[40] Boussac, A. and Rutherford, A.W. (1988) FEBS Lett. 236, 432–436.
[41] Tso, J., Sivaraja, M. and Dismukes, G.C. (1991) Biochemistry 30, 4734–4739.
[42] Mei, R. and Yocum, C.F. (1991) Biochemistry 30, 7836–7842.
[43] Boussac, A., Zimmermann, J.-L. and Rutherford, A.W. (1990) FEBS Lett. 277, 69–74.
[44] Surewicz, W.K. and Mantsch, H.H. (1988) Biochim. Biophys. Acta 952, 115–130.
[45] Miyazawa, T., Shimanouchi, T. and Mizushima, S. (1958) J. Chem. Phys. 29, 611–616.
[46] Byler, D.M. and Susi, H. (1986) Biopolymers 25, 469–487.
[47] Boussac, A., Zimmermann, J.-L., Rutherford, A.W. and Lavergne, J. (1990) Nature 347, 303–306.